CHAPTER V
PVDF/BST PIEZOELECTRIC COMPOSITES

5.1 Abstract

Fabrication of PVDF-$Ba_{0.7}Sr_{0.3}TiO_3$ composite film was used to extend the range of material properties. By adding $Ba_{0.7}Sr_{0.3}TiO_3$ ceramic powder into the polyvinylidene fluoride (PVDF) matrix, the piezoelectric composite was aimed to increase the dielectric and piezoelectric properties. Barium strontium titanate ($Ba_{0.7}Sr_{0.3}TiO_3$) was prepared via sol-gel method. The crystal structure of calcined $Ba_{0.7}Sr_{0.3}TiO_3$ at 1000°C was investigated by XRD which showed that $Ba_{0.7}Sr_{0.3}TiO_3$ belong to barium titanate perovskite structure. Sintered $Ba_{0.7}Sr_{0.3}TiO_3$ at 1330°C was found to be determinate by the response with curie point at 40°C. The composite film at different weight fraction of 0.2, 0.4 and 0.6 of barium strontium titanate ($Ba_{0.7}Sr_{0.3}TiO_3$) powder were prepared by compression molding into 250-300 μm thick sheets. DSC thermograms indicated that higher thermal stability was obtained at the higher ceramic content. The microstructure of the composite was observed using SEM. The dielectric constant and the dissipation factor of composites at different %wt of ceramic were measured as a function of frequency and temperature using Hewlett-Packard 4194A impedance/gain phase analyzer. The dielectric properties was revealed that the dielectric constant was enhanced at the higher $Ba_{0.7}Sr_{0.3}TiO_3$ ceramic content however the dielectric relaxaionwas still evident in polymer composite.

Keywords: PVDF/BST Composite; Dielectric properties

5.2 Introduction

The ceramic of bariums strontium titanate ($BaSrTiO_3$, BST) is a very attractive piezoelectric material for a large area of applications such as nonvolatile memories, surface acoustic wave devices, tunable capacitors, pyroelectric detectors, etc. bariums strontium titanate ($BaSrTiO_3$, BST), modificated from bariums titanate ($BaTiO_3$, BT). $BaTiO_3$ were attempted by substituting Sr for Ti and Ba [Ikeda, 1990

and Hui-dong *et al.*, 2004]. However, the preparation of $BaSrTiO_3$ is commonly involved with high temperature parameters or processes. Polyvinylidene fluoride (PVDF) is one of the most promising polymer materials for the piezoelectric and pyroelectric effects. The effects in PVDF have been observed since 1969 by Kawai, 1969 and Lang, 1971 respectively. The PVDF has low permittivity, low thermal conductivity and is flexible and relatively low in cost. Initial efforts were made in this work to extend the range of material properties which are desirable for applications by fabricating the composite comprising of $BaSrTiO_3$ and PVDF. Hu *et al.*, (2007) studied dielectric properties of BST/ cyclic olefin copolymer composite (COC). The composite shoed novel 0-3 type ceramic–polymer composite made of thermoplastic polymer with different loadings of ferroelectric barium strontium titanate (BST). The microstructures of the composites showed homogeneous distribution of the BST fillers in the COC polymer matrix in all the samples. The BSTn-COC composite with nanopowder showed higher relative permittivity and loss at BST loading over 10 vol.%. Using a 25% volume fraction of BST, a relative permittivity of 7.3 and a loss tangent of 0.0023 were obtained for the BSTn-COC nanocomposite at 1 GHz. Kohpaiboon *et al.*, (2007) studied composite film of PVDF and BST. BST nanopaticle was prepared via sol-gel method and PVDF/BST composite film was prepared using compression technique. They found much increasing of dielctric constant at all frequencies. The value increased with the BST ceramic content and also found that increasing temperature of calcine ceramic powders enhance the dielectric constant of composites.

The nano-sized $Ba_{0.7}Sr_{0.3}TiO_3$ has been prepared based on the sol-gel method. The PVDF/$Ba_{0.7}Sr_{0.3}TiO_3$ nanocomposite films were prepared using compression technique. Microstructure and distribution of ceramic power were observed by SEM. Higher thermal stabilities were found in composite film at higher ceramic content. Improvement of dielectric constant was obtained by adding $Ba_{0.7}Sr_{0.3}TiO_3$ ceramic into the PVDF matrix, the value was significantly increased from 5.9 of pure PVDF to 19.7, 23.8 and 34.3 of PVDF/BST20%, PVDF/BST40% and PVDF/BST60% respectively.

5.3 Experiment

5.3.1 Materials

Glacial acetic acid and methyl alcohol were purchased from Italmar. The Poly(vinylidene fluoride) (PVDF) pellets were given by Solvay (#1008). Barium acetate and *N,N*-Dimetyl formamide (DMF) were purchased from Lab Scan. Strontium acetate (99.995%) and titanium tetra-n-butoxide (97%) were purchased from S.M. Chemical.

5.3.2 Barium Strontium Titanate Preparation

$Ba_{0.7}Sr_{0.3}TiO_3$ powder was prepared by sol-gel process. Equal moles of barium acetate and strontium acetate were dissolved separately into methyl alcohol 20 ml in the presence of glacial acetic acid 10 ml. The solutions were then mixed and stirred for 20 minutes at room temperature. The prescribed amount of titanium-n-butoxide was added into the mixture. All the materials mentioned above were thoroughly mixed to prepare a stable solution with uniform composition until gel solution occurs. After that the gel solution was poured into an alumina crucible and heated by using a 2-step thermal decomposition method with calcining temperature of 1000°C in order to decompose the precursors and to crystallize the barium strontium titanate and investigate the dielectric properties of composites.

5.3.3 PVDF/Barium Strontium Titante Composite Preparation

PVDF pellets was dissolved in dimethyl formamide (DMF) at 60°C. For composite preparation the polymer/solvent ratio was 10g/100 ml. Proportionate quantity of $Ba_{0.7}Sr_{0.3}TiO_3$ powder was added in the polymer solution. It was homogenized by magnetic stirrer. Additional mixing by ultrasonic was used to guarantee that the powder agglomerated were broken. The solution was dried by heating at 100°C. The composite film was prepared by a Labtech compression as pressing dried solution at 200°C for 20 minutes under pressure of 15 tons. The thickness of the prepared films was ranged between 250-300 μm. Following the above method, the composite films of 20, 40 and 60% by weight ceramic were fabricated.

5.3.4 Characterization

Crystal structure of ceramic was characterized by X-ray diffraction (Rigaku, model Dmax 2002). The distribution of ceramic powders in composites was

observed using scanning electron microscope (SEM; LS002, JEOL). Thermal stabilities of composite film were investigated by Thermogravimetric Analyzer, (Q50 TGA). The piezoelectric properties were investigated by using RT66A and stress piezoelectric coefficients (d_{33}) of the polarized films were obtained from d_{33} meter (APC Int. Ltd., model 8000) operating at frequency of 1000 Hz and a time interval of 24 h after film polarization. The dielectric properties of composites were measured using Hewlett-Packard 4194A impedance/gain phase analyzer. The measurements were performed with a frequency range of 1 kHz-1 MHz.

5.4 Results and discussion

5.4.1 Barium Strontium Titanate ($Ba_{0.7}Sr_{0.3}TiO_3$)

5.4.1.1 X-ray diffraction XRD

Figure 5.1 showed the XRD spectral of calcined $Ba_{0.7}Sr_{0.3}TiO_3$ at 1000°C before sintering. XRD pattern showed sharp peaks around 32°, 40° and 45° [Choa *et al.*, 2004] which belong to the barium titanate perovskite structure. The XRD peak at $2\theta \sim 46^{\circ}$ show no splitting of $Ba_{0.7}Sr_{0.3}TiO_3$ which was indicated that $Ba_{0.7}Sr_{0.3}TiO_3$ is cubic structure [Ioachim *et al.*, 2007].

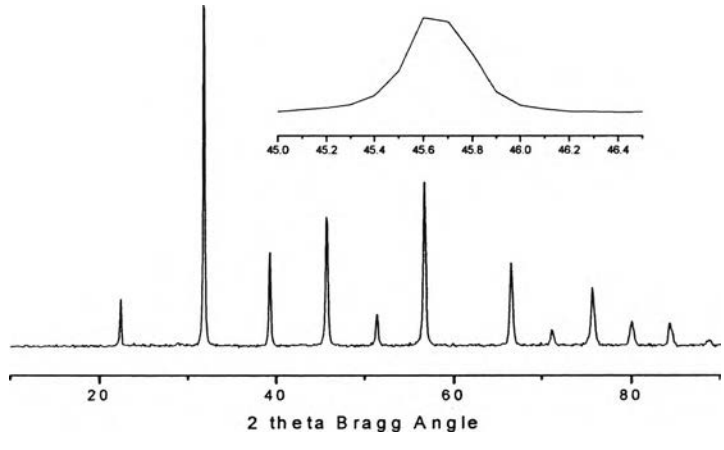

Figure 5.1 X-ray diffraction patterns of calcined $Ba_{0.7}Sr_{0.3}TiO_3$ at 1000 °C.

The cubic structure of $Ba_{0.7}Sr_{0.3}TiO_3$ could be confirmed by calculated lattice parameters as shown in Table 4.3.

Table 5.1 Lattice parameter of the calcined $Ba_{0.7}Sr_{0.3}TiO_3$ at 1000°C

Unit cell parameter		Unit cell volume	Tetragonal
a_0(nm)	c_0(nm)	v_0 x10^3(nm^3)	ratio c_0/a_0
0.397095	0.396965	59.32	0.999674

The $Ba_{0.7}Sr_{0.3}TiO_3$ powder after sintered at 1330°C reveals tetragonal phase as observed by the splitting at 2θ ~ 46° with tetragonality c_0/a_0 ≈1.001 as shown in Table 5.2. the XRD peaks at 2θ value between 44° and 47° is the (2 0 0) peaks are of a symmetric shape, indicating the cubic lattice for BST ceramic [Wie *et al.*, 2008]. It should be noted that, splitting of (2 0 0) peak indicated strontium ion Sr^{2+} enters substitutionally for Ba^{2+} ion in the lattice, and decreases considerably the tetragonal distortion of the unit cell. This can be explained from the fact that $Ba_{0.7}Sr_{0.3}TiO_3$ shows tetragonal after sintering process. This results could be confirmed by lattice parameter in table 5.2 and may be explained by the atomic entities must have been in the non-equilibrium position which relaxes to the equilibrium position when annealed at high temperature.

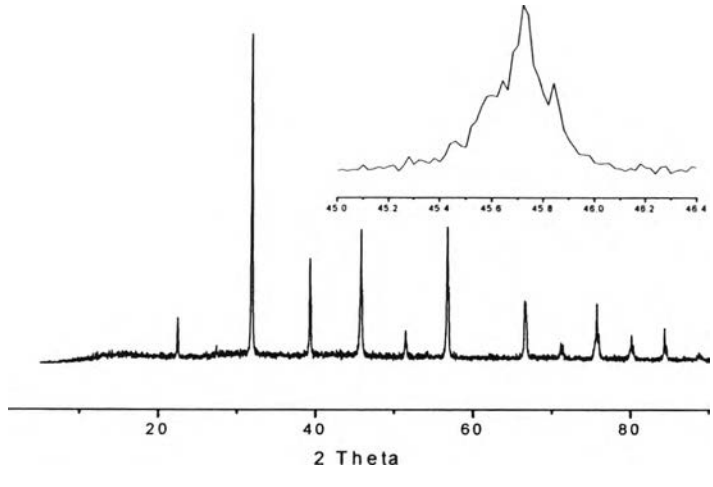

Figure 5.2 X-ray diffraction patterns of sintered $Ba_{0.7}Sr_{0.3}TiO_3$ at 1330°C.

Table 5.2 Lattice parameter of the sintered $Ba_{0.7}Sr_{0.3}TiO_3$ at 1330°C

Unit cell parameter		Unit cell volume	Tetragonal
a_0(nm)	c_0(nm)	v_0 x10^3(nm^3)	ratio c_0/a_0
0.396964	0.39749	62.63	1.001

5.4.1.2 Scanning Electron Microscopes (SEM) of sintered BST pellets)

The morphology of grains and the porous structure of BST ceramics were investigated by SEM. The typical micrographs of the microstructures of $Ba_{0.7}Sr_{0.3}TiO_3$ ceramic sintered at 1330°C showed the particle coalesce to form large well defined crystallite and the grain size of $Ba_{0.7}Sr_{0.3}TiO_3$. It can be seen that exaggerated particle growth with the development of interparticle necks thus resulting in particle fusion. The sintering process can be described as follows. When a powder material is compacted into a shape, the particles are in contact with one another at numerous sites, with a significant amount of pore space between them. In order to reduce the boundary energy atoms diffuse to the particle boundary areas, permitting the particles to be bonded together, and eventually causing the pores to shrink. If sintering is carried out for a long time, the pores may be eliminated and the material becomes dense [Guo *et al.*, 2004]

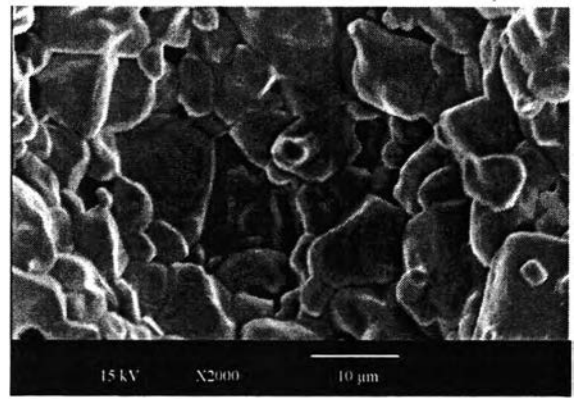

Figure 5.3 Scanning electron microscope (SEM) of the sintered $Ba_{0.7}Sr_{0.3}TiO_3$ at 1330°C.

5.4.1.3 Transmission Electron Microscopes (TEM)

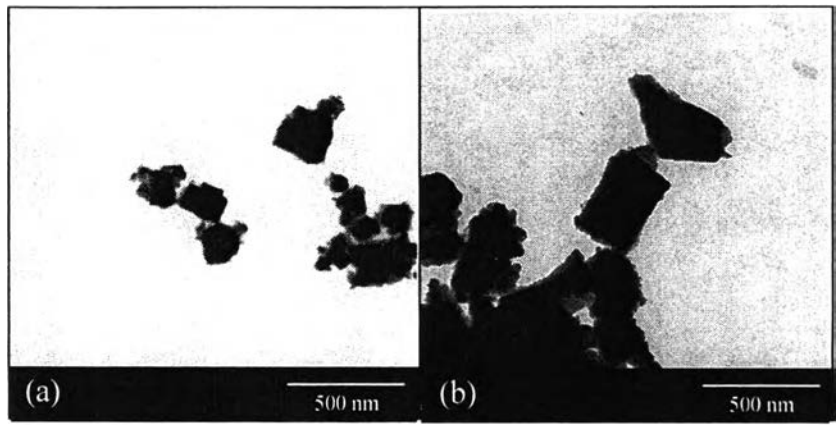

Figure 5.4 Transmission electron microscopes (TEM) of (a) calcined $Ba_{0.7}Sr_{0.3}TiO_3$ and (b) sintered $Ba_{0.7}Sr_{0.3}TiO_3$ at 1330°C for 2 h.

Figure 5.4 showed the particle size of $Ba_{0.7}Sr_{0.3}TiO_3$ investigated by TEM. The larger particle size was observed in sintered $Ba_{0.7}Sr_{0.3}TiO_3$ particles. Diameters of calcined $Ba_{0.7}Sr_{0.3}TiO_3$ and sintered particle $Ba_{0.7}Sr_{0.3}TiO_3$ were found to be approximately 50-100 nm and 100-200 nm respectively.

5.4.1.3 Dielectric Properties

Figure 5.5 shows frequency dependence on dielectric constant and dielectric loss of sintered BST at room temperature. It can be seen that dielectric constant of BST had high value (above 2000). This is due to the dielectric constant was done at room temperature which near the curie point of $Ba_{0.7}Sr_{0.3}TiO_3$ (as shown in Figure 5.6). At frequency above 1 MHz, the dielectric constant drops rapidly and dielectric loss sharply increases which indicates that the conductivity mechanism that might yields from the sample defect.

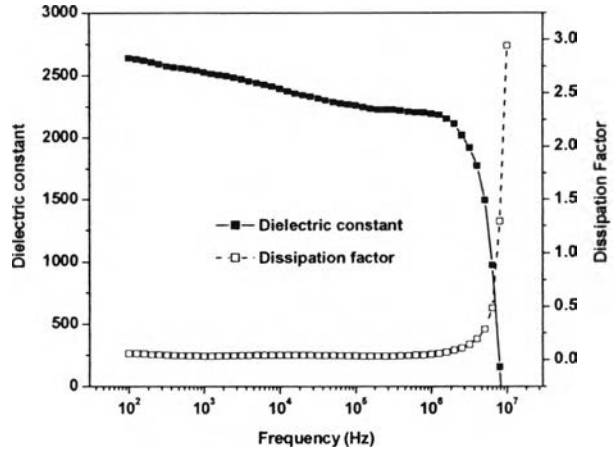

Figure 5.5 The frequency dependence of the dielectric constant and dissipation factor at room temperature of sintered $Ba_{0.7}Sr_{0.3}TiO_3$ at 1330°C.

The effects of temperature on the dielectric constant of the ceramics were also investigated. Figure 5.6 (a) showed the variation of dielectric constant of the $Ba_{0.7}Sr_{0.3}TiO_3$ ceramics with temperature at different frequency. The $Ba_{0.7}Sr_{0.3}TiO_3$ ceramic showed a peak at 40°C indicated curie temperature as a phase transition from ferroelectric to paraelectric phase [Kohpaiboon *et al.*, 2007] Therefore, the $Ba_{0.7}Sr_{0.3}TiO_3$ ceramic can use in ferroelectric application at temperature up to 40°C. Figure 5.6 (b) showed the variation of dissipation factor of the $Ba_{0.7}Sr_{0.3}TiO_3$ ceramics with temperature at different frequency which was lower than 0.2 at all temperatures and all frequencies.

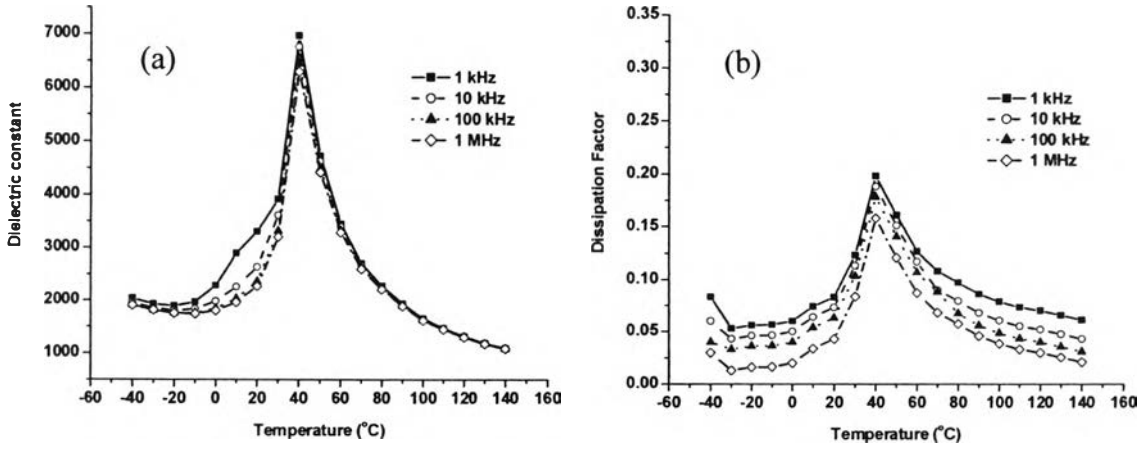

Figure 5.6 The temperature dependence of the dielectric constant and dissipation factor of sintered $Ba_{0.7}Sr_{0.3}TiO_3$ at 1330°C at different frequencies.

5.4.2 PVDF/Barium Strontium Titanate ($Ba_{0.7}Sr_{0.3}TiO_3$) composite film

5.4.2.1 Scanning Electron Microscopes (SEM) of PVDF-BST composite

SEM micrograph of the composites containing 20, 40, and 60 wt% ceramic filler which fine powder was dispersed in a PVDF matrix [Lu *et al.*, 2004] were shown in Figures 5.7. The composites displayed the microstructure of larger agglomeration in PVDF matrix when amount of ceramic increased. However at higher ceramic content, the flexibilities of composite films were reduced due to the high stiffness of ceramic powder.

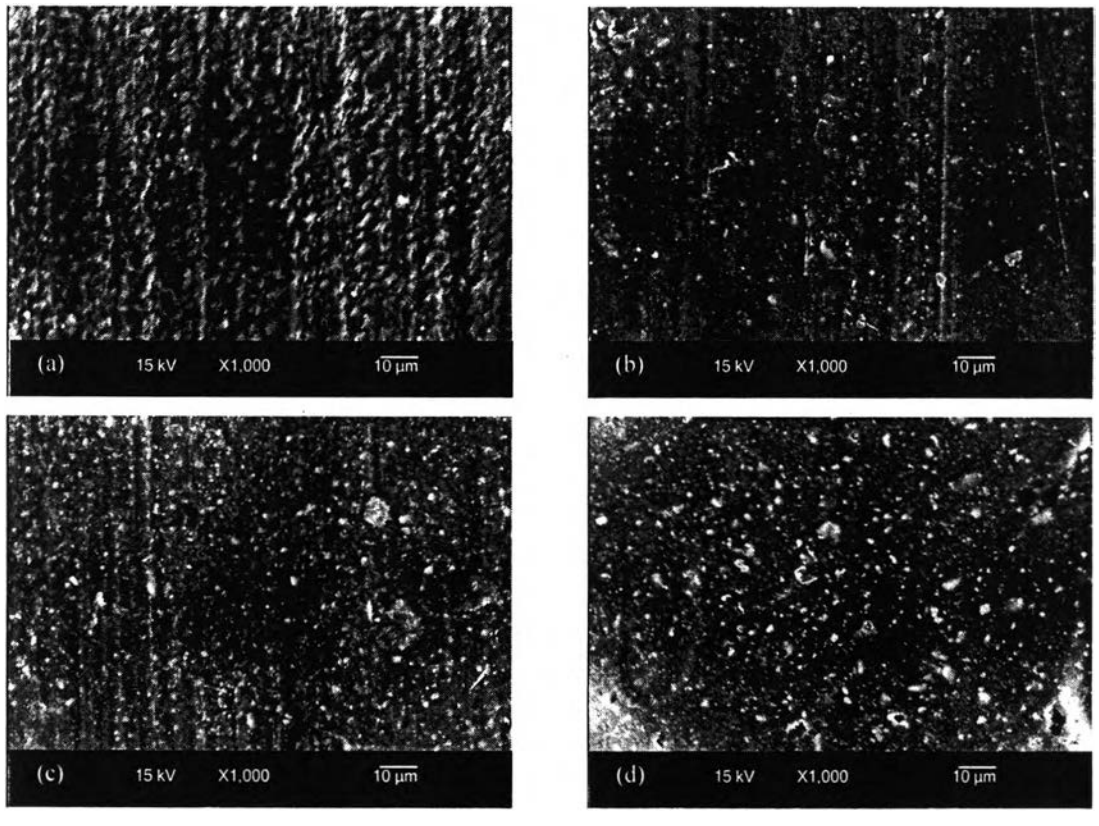

Figure 5.7 SEM micrographs of (a) compressed PVDF, (b) PVDF/BST20%, (c) PVDF/BST40% and (d) PVDF/BST60%.

5.4.2.2 Thermogravimetric Analysis-TGA

The graphic of weight loss versus temperature for PVDF and PVDF/$Ba_{0.7}Sr_{0.3}TiO_3$ composite as shown in Figure 5.8. The sharp decrease of weight loss was observed near 400°C due to the degradation of PVDF polymer. TGA

thermograms of PVDF/$Ba_{0.7}Sr_{0.3}TiO_3$ composites, in weight proportions of PVDF PVDF/BST20%, PVDF/BST40% and PVDF/BST60% in Figure 5.6 and Table 5.3 showed that the incorporation of $Ba_{0.7}Sr_{0.3}TiO_3$ in the PVDF films enhances the higher thermal stability of composite when compared to the pure PVDF.

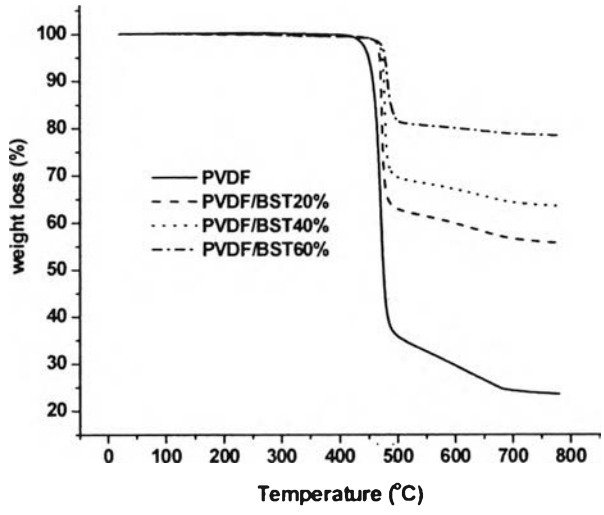

Figure 5.8 Weight loss (%) in function of the temperature (° C) for compressed PVDF and composite films.

Table 5.3 Decomposition of PVDF/$Ba_{0.7}Sr_{0.3}TiO_3$ at different % weight

Sample	Degradation temperature (Onset, °C)	Residual char (%w)
PVDF	457.51	23.5
PVDF/BST20%	469.17	55.6
PVDF/BST40%	473.69	63.5
PVDF/BST60%	475.98	78.4

5.4.2.3 Dielectric Properties

Dielectric constant and dissipation factor as the frequency range of 1 to 1 MHz of PVDF/BST composite film in various amount of BST ceramic were shown in Figure 5.9. The film, containing higher BST ceramic content yielded higher dielectric constant at all frequencies because of the high dielectric constant of $Ba_{0.7}Sr_{0.3}TiO_3$. However, at higher BST amount, the composite film showed higher

dielectric constant than that of pure PVDF film but the dissipation factor was significantly higher because the higher agglomeration of BST ceramic (as shown in Figure 5.7) yielded higher gap between polymer matrix and ceramic powder in composite films lead to higher dissipation factor when compare with the lower BST amount as shown in Figure 5.9 (b).

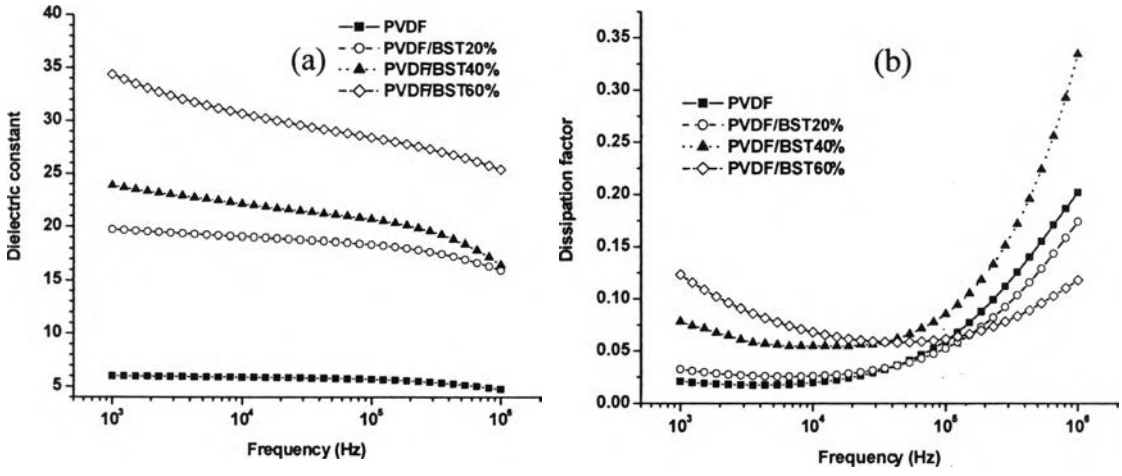

Figure 5.9 (a) Dielectric constant and (b) dissipation factor as the function of frequency of PVDF and PVDF/BST composite film at 20%, 40% and 60% by weight BST at room temperature.

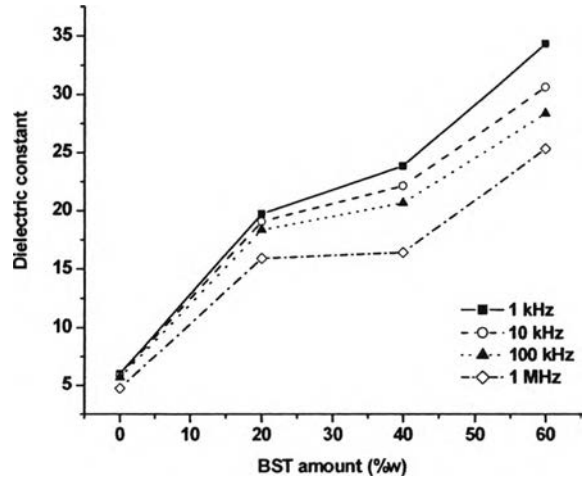

Figure 5.10 Dielectric constant at various amount of BST at 1 kHz, 10 kHz, 100 kHz and 1 MHz.

Figure 5.10 showed dielectric constant of PVDF/$Ba_{0.7}Sr_{0.3}TiO_3$ composite film, made from compression molding technique in various amount of BST ceramic. The figure showed that the dielectric constant was greater at higher amount of BST ceramic at all frequencies as seen from table 5.4.

Table 5.4 Dielectric constant of PVDF/BST composite film

PVDF/BST	Dielectric constant			
	1 kHz	10 kHz	100 kHz	1 MHz
0% BST	5.99	5.87	5.66	4.73
20% BST	19.73	19.07	18.34	15.92
40% BST	23.87	22.14	20.69	16.41
60% BST	34.35	30.67	28.39	25.36

The temperature dependent of dielectric constant of compressed PVDF film and PVDF/$Ba_{0.7}Sr_{0.3}TiO_3$ composites at the different amount of BST ceramic were investigated from -40°C to 140°C in Figure 5.11-5.14. From these graphs, it should be observed that the dielectric constant of all film increased rapidly from -40°C to 0°C and remained stable in the short range of temperature (0 ° C to 60°C) before shot up again at 70°C. Although $Ba_{0.7}Sr_{0.3}TiO_3$ was added into the PVDF, the pattern of dissipation factor of all samples showed almost the same as the pure PVDF film which refer that the molecular relaxation of PVDF film which has two loss mechanism (in temperature range of -40°C to 140°C) influent to dissipation factor of the composite film more than the relaxation of $Ba_{0.7}Sr_{0.3}TiO_3$ ceramic (indicate relaxation peak at 40°C).

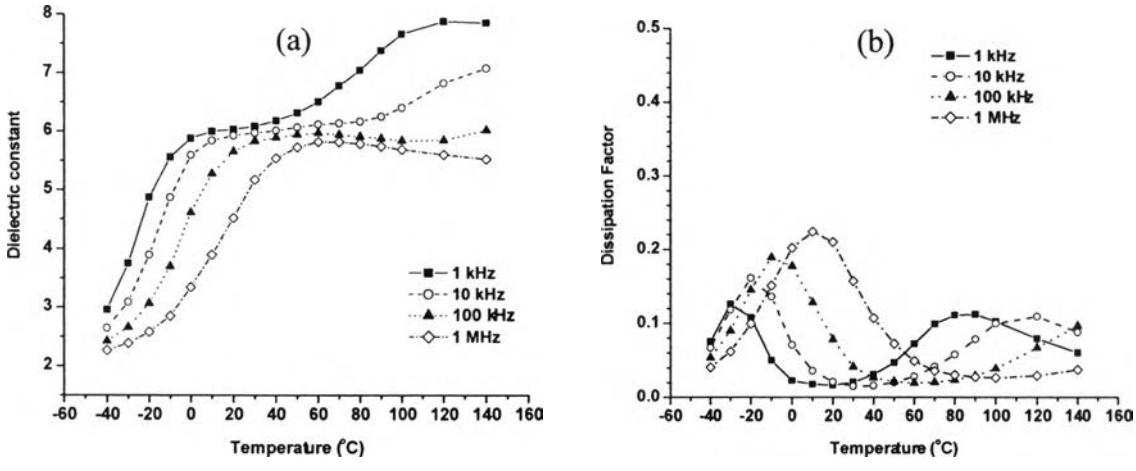

Figure 5.11 The temperature dependence of (a) the dielectric constant and (b) dissipation factor of compressed PVDF film at 1 kHz, 10 kHz, 100 kHz and 1 MHz.

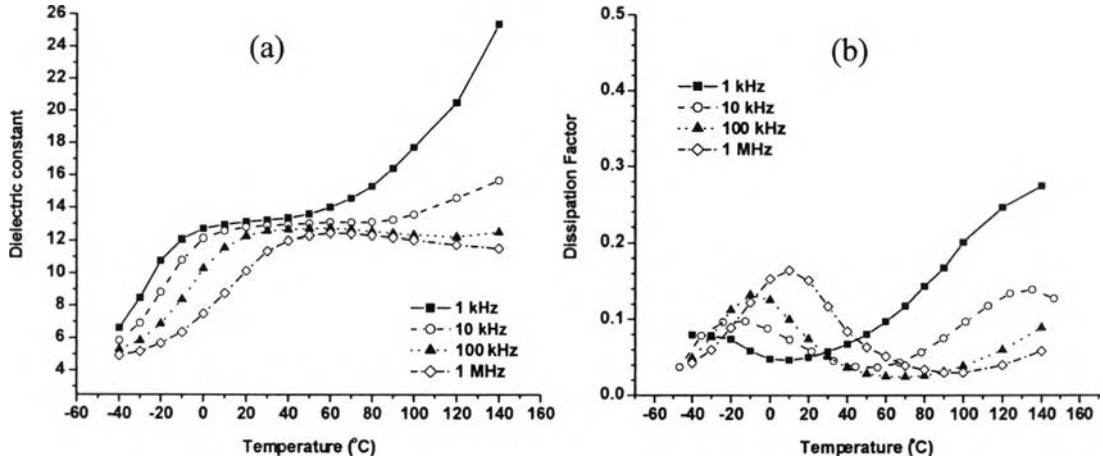

Figure 5.12 The temperature dependence of (a) the dielectric constant and (b) dissipation factor of PVDF/BST20% at 1 kHz, 10 kHz, 100 kHz and 1 MHz.

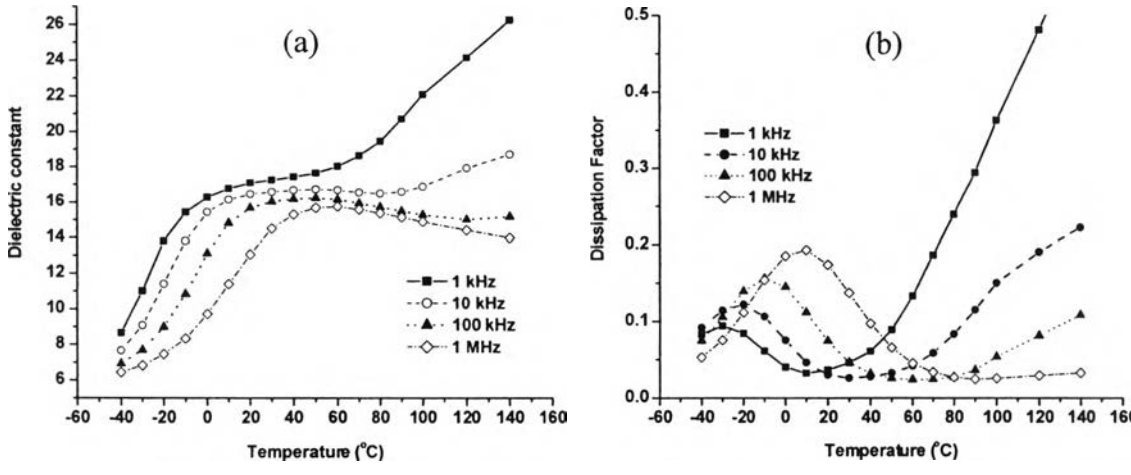

Figure 5.13 The temperature dependence of (a) the dielectric constant and (b) dissipation factor of PVDF/BST40% at 1 kHz, 10 kHz, 100 kHz and 1 MHz.

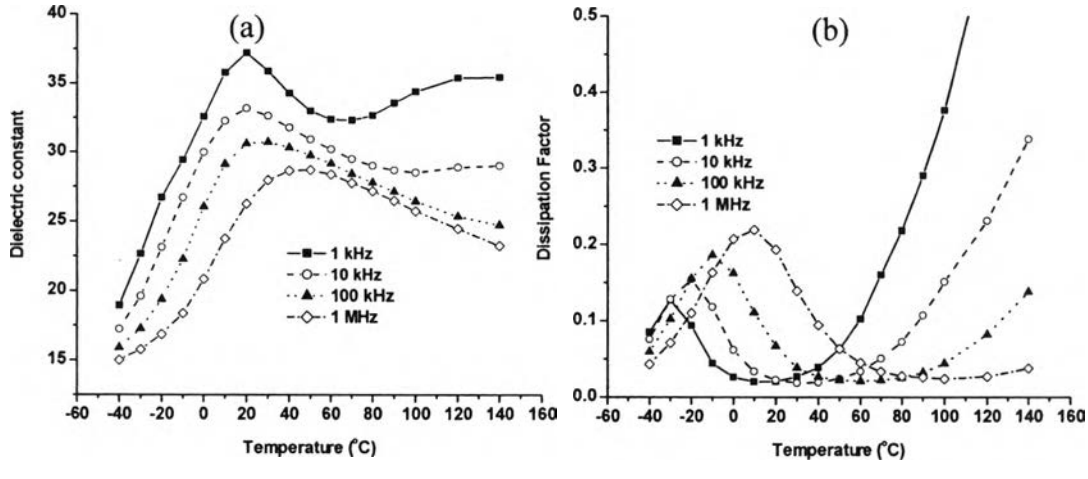

Figure 5.14 The temperature dependence of (a) the dielectric constant and (b) dissipation factor of PVDF/BST60% at 1 kHz, 10 kHz, 100 kHz and 1 MHz.

5.5 Conclusion

The PVDF/ $Ba_{0.7}Sr_{0.3}TiO_3$ composite were successfully fabricated. The high content of $Ba_{0.7}Sr_{0.3}TiO_3$ in the composite shows enhancement of dielectric constant. However, more agglomeration of ceramic powder were found in composites at higher $Ba_{0.7}Sr_{0.3}TiO_3$ content which made them opaque and stiff resulting in high dissipation

factor. The molecular relaxation of composite film was observed as a dissipation factor by showing the dominant influence of PVDF at all ceramic contents. Also the thermal stability of the composites can be improved by higher amount of ceramic powders but melting temperature of composite does not change compared to pristine PVDF.

5.6 Acknowledgements

The authors would like to thank Dr. Pitak Laoratanakul and MTEC staffs for useful assistance and instruments for characterizations. The partial funding of research work was provided by the National Center of Excellence for Petroleum, Petrochemicals, and Advanced Materials, Thailand. And Polymer Processing and Nanomaterials research unit.

5.7 References

Cho, S.D., Lee, J.Y., Hyuna, J.G., Paik, K.W. (2004) Study on epoxy/$BaTiO_3$ composite embedded capacitor films (ECFs) for organic substrate applications. Materials Science and Engineering B, 110, 233-239.

Guo, H., Gao, W. and Yoo, J. (2004) Barium strontium titanate ($Ba_{0.7}Sr_{0.3}TiO_3$) ferroelectric films produced by electrophoretic deposition. Current Applied Physics 4, 385–388

Hu, T., Juuti, J., Jantunen H. and Vilkman, T. (2007) Dielectric properties of BST/polymer composite. Journal of the European Ceramic Society, 27, 3997–4001.

Hui-dong, L., Chu-de, F. and Wen-long, Y. (2004) Some effects of different additives on dielectric and piezoelectric properties of $(Bi_{1/2}Na_{1/2})Tio_3$-$BaTiO_3$ morphotropic-phase-boundary composition. Materials Letters, 58, 1194-1198.

Ikeda, T. (1990) Fundamental of piezoelectricity, Oxford Science Publications. New York.

Ioachim, A., Ramerb. R., Toacsan, M.I., Banciu, M.G., Nedelcu, L., Dutu, C.A., Vasiliu, F., Alexandru, H.V., Berbecaru C., Stoica, G., Nita, P. (2007) Ferroelectric ceramics based on the BaO–SrO–TiO_2 ternary system for microwave applications. Journal of the European Ceramic Society 27, 1177–1180

Kawai, H. (1969) The Piezoelectricity of Polyvinylidene Fluoride. Japan Journal of Applied Physics, 8, 975-976.

Kohpaiboon, K., and Manuspiya, H.,(2007) 0-3 Connectivity of PVDF/BST Piezoelectric Composites M.S. thesis, The Petroleum and Petrochemical College, Chulalongkorn University, Bangkok, Thailand.

Lang, S.B. 1971. Ferroelectrics, Physical Review Letter, B 4 : 3603.

Lu, Q., Chen, D. and Jiao, X. (2003) Preparation and characterization of Ba SrTiO (x=0.1, 0.2) fibers by sol–gel process using catechol-complexed titanium isopropoxide, Journal of Alloys and Compounds, 358, 76–81.

Wei, X., Xu, G., Ren, Z., Wang, Y., Shen, G. and Han, G. (2008) Composition and shape control of single-crystalline $Ba_{1-x}Sr_xTiO3$ (x = 0–1) nanocrystals via a solvothermal route. Journal of Crystal Growth, 310, 4132-4137.